PAPER • OPEN ACCESS

A practical design procedure for initial sizing of heaving point absorber wave energy converters

To cite this article: M B Jouybari and Y Xing 2021 *IOP Conf. Ser.: Mater. Sci. Eng.* **1201** 012018

View the article online for updates and enhancements.

A practical design procedure for initial sizing of heaving point absorber wave energy converters

M B Jouybari and Y Xing*

University of Stavanger, Norway

* Contact author: yihan.xing@uis.no

Abstract. Designing a wave energy converter with the proper size has always been challenging since it is a trade-off between many factors including cost, practicality, and energy output. In this paper a practical design procedure for sizing of heaving point absorbers wave energy converters is presented. Size can be represented by the body volume. Budal power bounds are deployed to obtain the body volume and annual mean absorbed power of the wave energy converter. Budal power bounds are determined for each sea state. Aiming a specific power capture ratio, several sets of design sea states with related design volume and annual mean absorbed power are defined. With the design objective of maximizing the ratio of mean power to submerged volume, and considering suitable design constraints, the best size is obtained. The proposed procedure will be then deployed for a case study and the design will be compared with an existing similar point absorber. The results show that the mean absorbed power does not depend on the size but is a function of selected sea states. Furthermore, the comparison study reveals that the proposed design procedure yields reasonable power characteristics.

1. Introduction and background

One of the main considerations in designing wave energy converters is determining their size. A wave energy converter (WEC) should be sized to fulfil the power requirements. The design should be practical; in other words, very small or very large bodies are not practical. There have been several works on the size and geometry study of WECs in the literature; most of which are on size comparison or size optimization. In some early studies by Kan [1], Haren and Mei [2] and Thomas and Gallagher [3], geometry and size were studied with respect to the power maximization attitude. In more advanced works by Babarit et al. [4], multi objective optimization study was conducted to maximize the power and minimize the total mass. McCabe et al. [5] also optimized the shape of the WEC with the objectives including power, submerged volume, and velocity. It is reported by Bachynski et al. [6] that the idealized power take-off damping increases with the increase in the size of WEC. With the main objective of finding the best location for utilizing the point absorbers, Khojasteh et al. [7] studied the effects of the buoy draft and diameter to determine the maximum power absorption and concluded that the buoy diameter has a significant effect on the captured power while the power absorption was smaller for larger drafts. More importantly, the absorbed power depends highly to the significant wave height. Similarly, Shadman et al. [8] proposed a methodology for the geometrical optimization of heaving point absorbers. They considered the diameter and draft of the buoy as geometrical parameters to be determined in order to achieve a maximized combination of the absorbed power and the resonance bandwidth of the buoy. A preliminary design of point absorbers by using a parametric optimization study aiming to capture the

maximum energy in a target area was proposed by Erselcana İ Ö and Kükner A [9]. They considered a broad range of design variables and commented on the performance of WECs with different floated shapes. They also mentioned that increasing the floater mass has a trivial effect on the energy capture.

Knowing the optimized body size and geometry is useful, but one important issue is missing in the above-mentioned references which is that it is essential to know how the WEC's size for specific power purposes can be determined. In a study on developing heaving point absorbers that maximize the power output, Falnes et al. [10] drew a promising conclusion that the capacity of the power take-off (PTO) system, and the maximum volume should be limited. They assumed that a commercially practical WEC should work at least one-third of the year with full capacity, derived the corresponding maximum power and used that to size the WEC. This in general leads to a lower specific power level which in turn calls for a smaller WEC volume. Furthermore, they stated that instead of having a very large power buoy, a reasonable wave-power plant should be made of an array of many small power units. They applied the Budal diagrams [11] and investigated the power output with respect to the WEC's volume and suggested that the parameters of the WEC should be matched with the wave climate. A more detailed investigation of the arrays of point absorbers was conducted by Murai et al. [12]. They derived optimal control force parameters to maximize power generation of multi point-absorber arrays, studied different arrangements of the arrays, and concluded that the optimized array arrangement increases the power generation efficiencies by 15%.

Despite several valuable research on the size of WECs, there is yet a need for a design procedure on sizing that can be conveniently applied for initial sizing purposes. This will be proposed in this paper. In the proposed method, Budal upper bounds are implemented to characterize the absorbed power to provide a practical initial sizing of heaving point absorbers. In this paper, first, the sizing procedure is presented in Section 2.   along with the implemented methods. Second, to have a better understanding of the sizing procedure, it is performed on a case study of point absorbers in a specific sea site and sea states which is introduced in Section 3. Third, the results are presented, compared with an existing similar point absorber, and discussed in Section 4. Lastly, conclusions are given in Section 5.

2. Theory and methodology

2.1. Assumptions
The following assumptions are made:
- It is assumed that the design wave height (H_{design}) and design wave period (T_{design}) are equal to significant wave height (H_s) and spectral peak period (T_p), respectively. This is because for a given sea state, H_s is an indication of the wave energy and T_p is the wave period of the most energetic waves in the total wave spectrum.
- Only the left-hand Budal curve is considered for power calculation (Section 2.4.). With a fixed design volume, the power is only a function of wave height and period which are equal or less than the H_{design}, and T_{design}, hence the power follows the left hand Budal curve.
- The intersection of the left-hand Budal curve and right-hand curve is used to calculate the volume (Section 2.4. 2.5. 2.5.).
- The PTO system is ideal, i.e., the wave energy absorbed will follow the upper limits of the Budal diagram.

2.2. The design procedure
The design workflow is summarized in Figure 1.
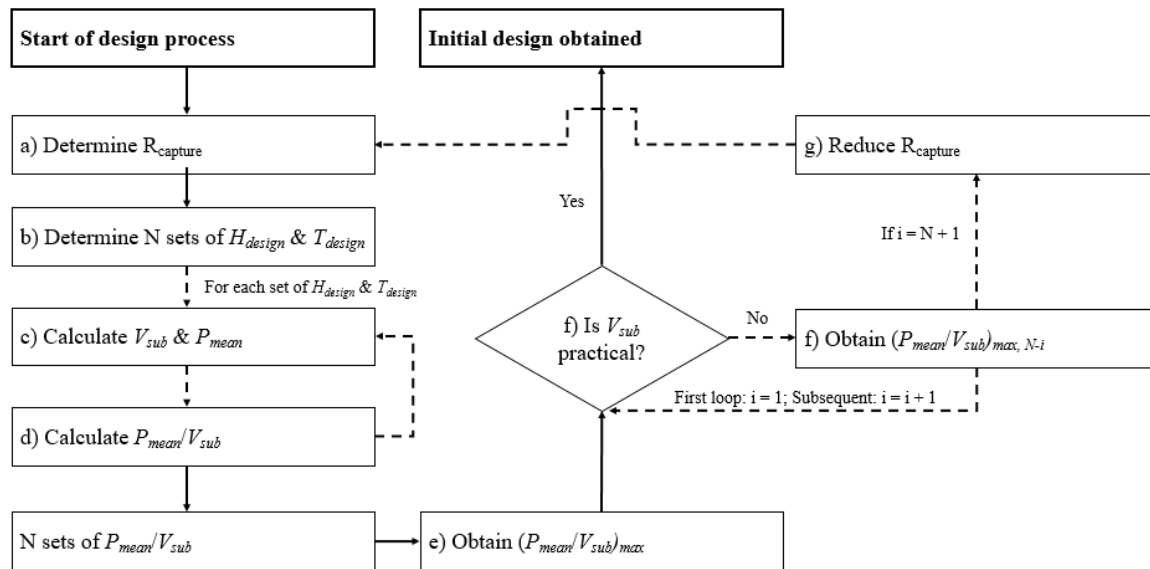
Figure 1. Size design workflow.

The design procedure consists of the following steps:

a)   First, the power capture ratio is determined. This is the percentage of the sea power that the WEC is designed to capture and defines the sea states domain or target sea states (Section 2.3).

b)   From the sea states, sets of H_{design} and T_{design} corresponding to the determined power capture ratio are determined.

c)   For each set of H_{design} and T_{design}, the design submerged volume (V_{sub}) is calculated.

d)   The ratio of annual mean absorbed power to the submerged volume (P_{mean}/V_{sub}) is calculated for each set.

e)   The maximum P_{mean}/V_{sub} is obtained.

f)   If the volume corresponding to this maximum ratio of P_{mean}/V_{sub} is practical, the initial sizing is obtained. Otherwise, the next maximum ratio should be investigated until a practical size is found.

g)   If none of the investigated cases result in a practical volume then the capture ratio should be modified to a lower percentage.

2.3. Power capture ratio

The power capture ratio determines the sea states to which the WEC is designed to function and is defined as follows:

$$capture\ ratio = P\left(T_{p,min} < t < T_{p,max}, H_{s,min} < h < H_{s,max}\right) \tag{1}$$

where $T_{p,min}$ and $T_{p,max}$ are respectively the minimum and maximum wave periods and $H_{s,min}$ and $H_{s,max}$ are respectively the minimum and maximum wave heights corresponding to any point on the capture ratio plot. Sum of the probabilities of sea states within these limits is equal to the capture ratio. Equation (1) is visually represented as a box on the scatter diagram as presented in Figure 2.
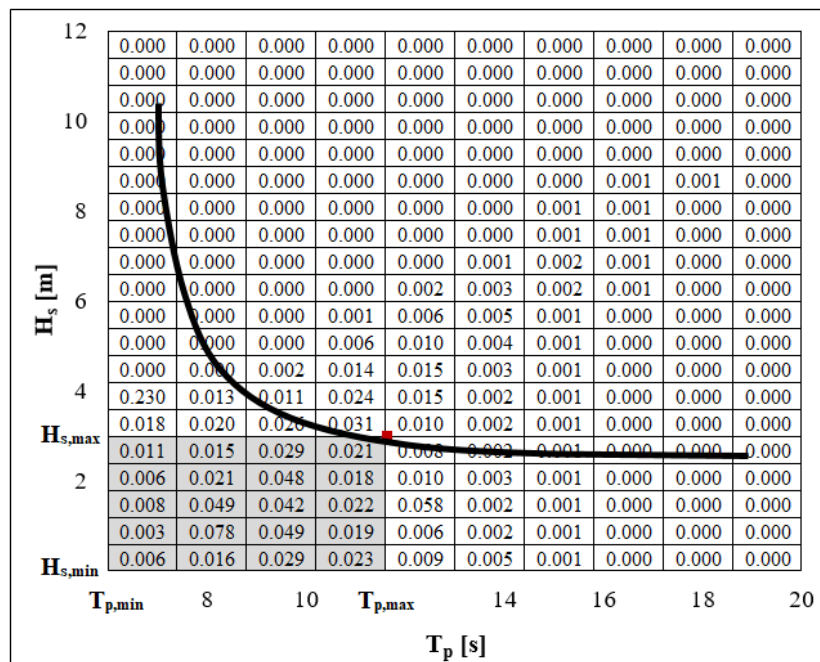
Figure 2. A schematic capture ratio plot and its corresponding sea states and probabilities.

2.4. Budal power upper bounds

The power and volume calculations in this study are based on Budal power bounds [13]. With an incident plane wave with the wave-power level J and wavelength λ, the left upper bound for the absorbed wave power for the heaving axisymmetric body in deep water will be defined as:

$$P < P_A \equiv c_A H^2 T^3 \tag{2}$$

where T and H are wave period and wave height, respectively.

This upper bound does not depend on the size but depends on the body's shape and oscillation mode. The right upper bound to the power that can be absorbed by an immersed body oscillating in heave with the volume, V, can be defined as:

$$P < P_B \equiv c_B \frac{VH}{T} \tag{3}$$

These upper bounds are shown in Figure 3. The left-hand upper bound P_A is size-independent and the right-hand upper bound P_B is a function of body volume. However, both upper bounds are functions of H and T.
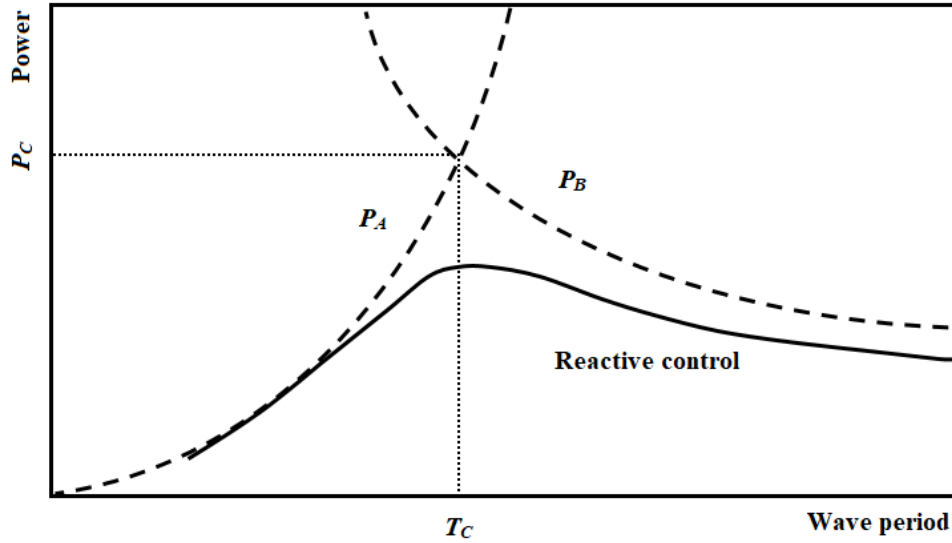
Figure 3. Budal upper bounds. The intersection of left-hand and right-hand curves (P_A and P_B) is defined by T_C and P_C.

2.5. The smallest required volume

Budal upper bounds are to be plotted for several sets of H_{design} and T_{design} along the capture ratio plot in Figure 2. Maximum absorbed power (P_{max}) is calculated by following the P_A curve in Figure 3 and using equation (4).

$$P_{max,design} = c_A H_{design}^2 T_{design}^3 \tag{4}$$

In practice, P_{max} is lower than the intersection-point power (P_C) due to the PTO system limitations. The P_{max}/P_C ratio is varied for different control strategies [14]. Therefore, the power curve and consequently the WEC's submerged volume should be calculated according to the applied PTO system. However, as mentioned earlier, this limitation is neglected in the present study and the PTO system is considered to be ideal.

For each set of H_{design} and T_{design}, and by setting $T = T_C = T_{design}$, the WEC's submerged volume can be determined:

$$V_{sub,design} = \frac{c_A H_{design} T_{design}^4}{c_B} \tag{5}$$

As well as the submerged volume, the annual mean absorbed power (P_{mean}) and the ratio of mean power to the submerged volume (P_{mean}/V_{sub}) are to be calculated. The calculation of P_{mean} is explained in Section 2.6.

2.6. Mean absorbed power

Each set of H_{design} and T_{design} represents a sea states domain with n subsets of H_s and T_p and their corresponding probabilities of occurrence. The sum of calculated mean power of all these subsets multiplied by their individual probabilities yields the P_{mean} of that design set through equation (6).

$$P_{mean,design} = \sum_{i=1}^{n} P_{mean,i} \times p_i \tag{6}$$

The P_{mean} of each subset is calculated from the P_A curve using equation (7).

$$P_{mean,i} = c_A \bar{H}_i^2 \bar{T}_i^3 \tag{7}$$

where $\bar{T}_i$ is the mean wave period of each subset, which is estimated using equation (8) by assuming that the waves follow a JONSWAP spectrum with first and zeroth moment of m_0 and m_1, respectively. $\bar{H}_i$ is the mean wave height of each subset, which is estimated by equation (9) by applying the Rayleigh probability distribution to random wave heights.

$$\bar{T}_i = \frac{m_{0,i}}{m_{1,i}} \tag{8}$$

$$\bar{H}_i = \sqrt{\frac{\pi}{8}} H_{s,i} \tag{9}$$

2.7. Capture width ratio (CWR)

The *CWR* is used to measure the capture efficiency of the WEC and can be used for comparison purposes. It is calculated by using equation (10).

$$CWR = \frac{C_W}{B} \tag{10}$$

where B is the characteristic dimension of the WEC and C_W is the capture width which is the ratio of mean absorbed power to the incident wave power resource (P_W) and is obtained by equation (11).

$$C_W = \frac{P_{mean}}{P_W} \tag{11}$$

where P_W or the power per meter of wave front for a sinusoidal wave is calculated by equation (12).

$$P_W = \frac{\rho_w g^2}{32\pi} H^2 T \approx 980 H^2 T \ (W m^{-1}) \tag{12}$$

3. Case Study

The environmental conditions of the European Marine Energy Centre (EMEC) test site [15] for the small bottom-referenced heaving buoy (Bref-HB) form is used as the case study. The site is located on the Orkney Islands in Scotland and its scatter diagram is presented in Table 1.

Table 1. Joint distribution scatter diagram of H_s and T_p of EMEC site [15].
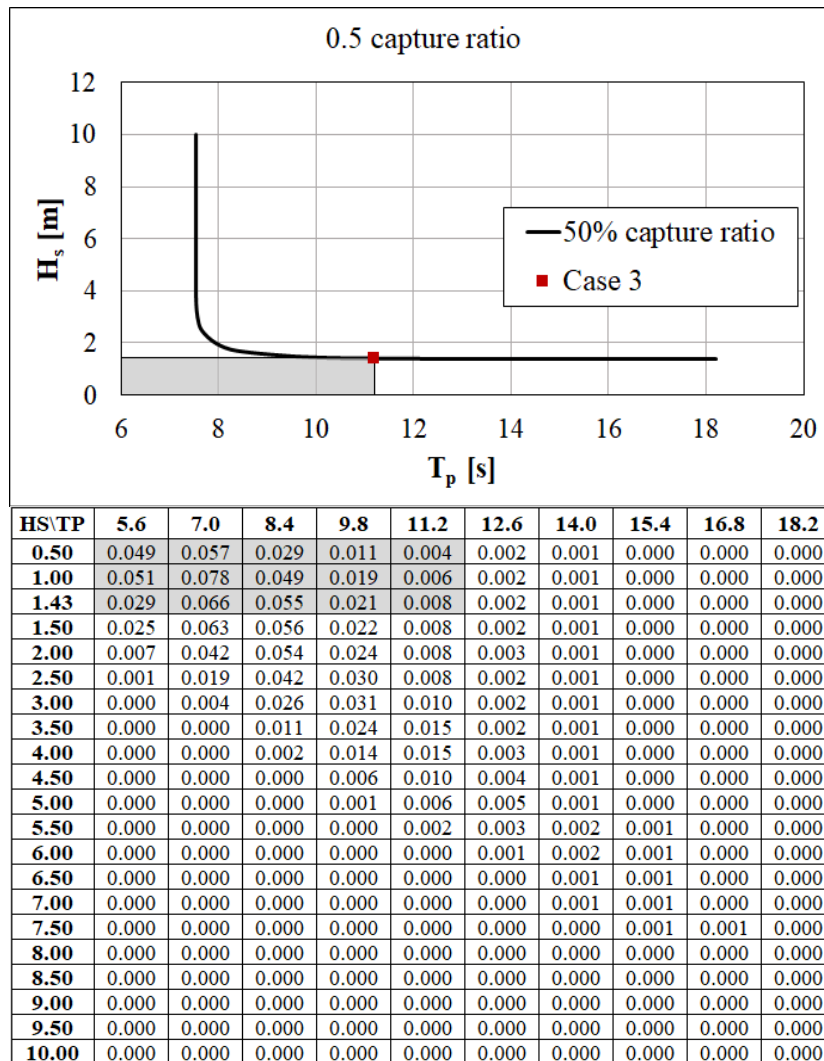
T_p / H_s	4.9-6.3	6.3-7.7	7.7-9.1	9.1-10.5	10.5-11.9	11.9-13.3	13.3-14.7	14.7-16.1	16.1-17.5	17.5-18.9	Marginal for H_s
0.00-0.75	393	455	233	87	33	14	6	2	0	0	119
0.75-1.25	408	629	391	151	52	15	6	2	0	0	1223
1.25-1.75	200	508	448	174	62	20	7	1	0	0	1654
1.75-2.25	54	338	433	193	61	22	9	2	0	0	1420
2.25-2.75	7	151	339	244	61	19	10	3	1	0	1112
2.75-3.25	1	29	211	252	80	16	7	3	1	0	835
3.25-3.75	0	3	91	191	118	19	5	2	1	0	600
3.75-4.25	0	0	17	114	119	25	5	2	1	0	430
4.75-4.75	0	0	1	49	78	36	6	2	1	0	283
4.75-5.25	0	0	0	11	46	42	7	2	1	0	173
5.25-5.75	0	0	0	1	18	26	15	7	0	0	109
5.75-6.25	0	0	0	1	1	7	18	11	1	0	67
6.25-6.75	0	0	0	1	1	2	9	10	2	0	39
6.75-7.25	0	0	0	0	0	0	5	9	4	0	25
7.25-7.75	0	0	0	0	0	0	2	7	5	0	18
7.75-8.25	0	0	0	0	0	0	1	4	4	1	14
8.25-8.75	0	0	0	0	0	0	0	1	2	1	10
8.75-9.25	0	0	0	0	0	0	0	1	2	1	4
9.25-9.75	0	0	0	0	0	0	0	0	1	1	4
9.75-10.25	0	0	0	0	0	0	0	0	0	1	1
Marginal for T_p	1063	2113	2164	1469	730	263	118	71	27	5	8023

4. Results and discussion

4.1. Solved example

The H_s-T_p plots corresponding to the 0.25 and 0.5 capture ratios are derived from the joint probability scatter diagram. Along each plot, 12 cases are selected for investigation. Figure 4 shows the 50 % capture plot as well as the case No. 3 and its corresponding probabilities.

| HS\TP	5.6	7.0	8.4	9.8	11.2	12.6	14.0	15.4	16.8	18.2
0.50	0.049	0.057	0.029	0.011	0.004	0.002	0.001	0.000	0.000	0.000
1.00	0.051	0.078	0.049	0.019	0.006	0.002	0.001	0.000	0.000	0.000
1.43	0.029	0.066	0.055	0.021	0.008	0.002	0.001	0.000	0.000	0.000
1.50	0.025	0.063	0.056	0.022	0.008	0.002	0.001	0.000	0.000	0.000
2.00	0.007	0.042	0.054	0.024	0.008	0.003	0.001	0.000	0.000	0.000
2.50	0.001	0.019	0.042	0.030	0.008	0.002	0.001	0.000	0.000	0.000
3.00	0.000	0.004	0.026	0.031	0.010	0.002	0.001	0.000	0.000	0.000
3.50	0.000	0.000	0.011	0.024	0.015	0.002	0.001	0.000	0.000	0.000
4.00	0.000	0.000	0.002	0.014	0.015	0.003	0.001	0.000	0.000	0.000
4.50	0.000	0.000	0.000	0.006	0.010	0.004	0.001	0.000	0.000	0.000
5.00	0.000	0.000	0.000	0.001	0.006	0.005	0.001	0.000	0.000	0.000
5.50	0.000	0.000	0.000	0.000	0.002	0.003	0.002	0.001	0.000	0.000
6.00	0.000	0.000	0.000	0.000	0.000	0.001	0.002	0.001	0.000	0.000
6.50	0.000	0.000	0.000	0.000	0.000	0.000	0.001	0.001	0.000	0.000
7.00	0.000	0.000	0.000	0.000	0.000	0.000	0.001	0.001	0.000	0.000
7.50	0.000	0.000	0.000	0.000	0.000	0.000	0.000	0.001	0.001	0.000
8.00	0.000	0.000	0.000	0.000	0.000	0.000	0.000	0.000	0.000	0.000
8.50	0.000	0.000	0.000	0.000	0.000	0.000	0.000	0.000	0.000	0.000
9.00	0.000	0.000	0.000	0.000	0.000	0.000	0.000	0.000	0.000	0.000
9.50	0.000	0.000	0.000	0.000	0.000	0.000	0.000	0.000	0.000	0.000
10.00	0.000	0.000	0.000	0.000	0.000	0.000	0.000	0.000	0.000	0.000

Figure 4. Top: 50% capture plot of sea states (black curve). The shaded area shows the corresponding sea states rectangle for the Case 3. Bottom: joint probability diagram and the shaded probabilities corresponding to Case 3.

The design V_{sub} and P_{mean} are calculated for each case using equations (5) and (6), respectively. Note that the coefficients c_A and c_B for an axisymmetric body in heave mode are taken as $c_A = 245\ Wm^{-2}s^{-3}$ and $c_B = \sigma\rho g = \sigma \times 10055\ Wm^{-4}s$ where $\sigma = 1$ for periodic oscillation [14]. The ratio of P_{mean}/V_{sub} can be calculated accordingly. The results are shown in Table 2. Moreover, Figure 5-Figure 7 show the changes of the P_{mean} and the P_{mean}/V_{sub} ratio with different design parameters.

Among the selected cases for 50% capture ratio, case number 6 (H_{design}=2.5 m, T_{design} = 7.7 s) has the highest P_{mean}/V_{design} ratio equal to 0.103 kW/m^3. The V_{sub} for this case is 209 m^3 and the P_{mean} is 21.5 kW. For 25% capture ratio, the best case is number 9 (H_{design}= 2 m, T_{design} = 6.3 s) with P_{mean}/V_{sub} of 0.073 kW/m^3, V_{sub} of 76 m^3, and P_{mean} equal to 5.5 kW.

**Table 2.** Performance measures and characteristics of design sets

Capture ratio (%)	Case No.	T_{design} (s)	H_{design} (m)	P_{max} (kW)	V_{sub} (m³)	P_{mean} (kW)	P_{mean}/V_{sub} (kW/m³)
50	1	18.2	1.4	2887	3737	14.0	0.004
	2	14.0	1.4	1320	1311	13.9	0.011
	3	11.2	1.4	699	546	13.2	0.024
	4	8.4	1.7	424	207	16.8	0.081
	5	8.0	2.0	493	195	16.7	0.086
	6	**7.7**	**2.5**	**687**	**209**	**21.5**	**0.103**
	7	7.6	3.0	957	240	23.8	0.099
	8	7.5	3.5	1289	276	24.7	0.089
	9	7.5	4.5	2126	354	24.9	0.070
	10	7.5	6.0	3779	472	24.9	0.053
	11	7.5	8.0	6719	630	24.9	0.040
	12	7.5	10.0	10498	787	24.9	0.032
25	1	18.2	0.7	802	1970	2.8	0.001
	2	12.6	0.7	268	454	2.7	0.006
	3	11.2	0.7	192	286	2.6	0.009
	4	9.8	0.8	135	172	2.5	0.015
	5	8.4	0.8	99	100	2.3	0.023
	6	7.3	1.0	94	68	3.5	0.051
	7	7.0	1.1	99	63	2.4	0.037
	8	6.5	1.5	150	65	4.0	0.062
	9	**6.3**	**2.0**	**244**	**76**	**5.5**	**0.073**
	10	6.2	2.5	371	92	6.3	0.069
	11	6.2	3.0	532	110	6.5	0.059
	12	6.2	10.0	5910	366	6.5	0.000
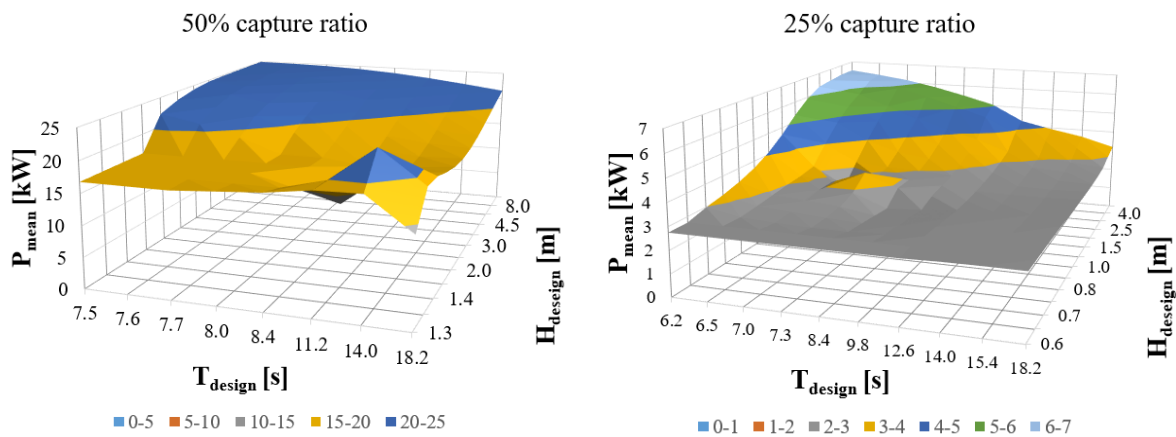
Figure 5. The changes of the P_{mean} with wave parameters. Left: 50% capture ratio. Right: 25% capture ratio.
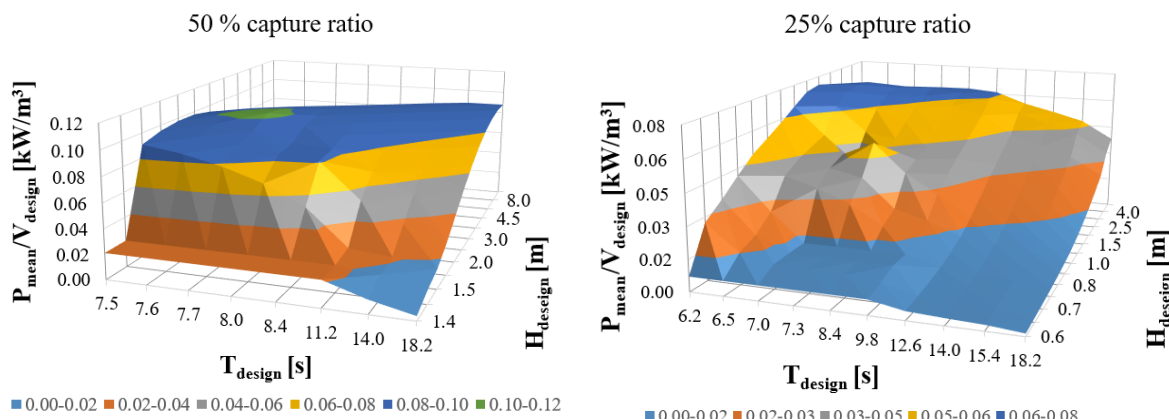
Figure 6. The changes of the P_{mean}/V_{sub} with wave parameters. Left: 50% capture ratio. Right: 25% capture ratio.
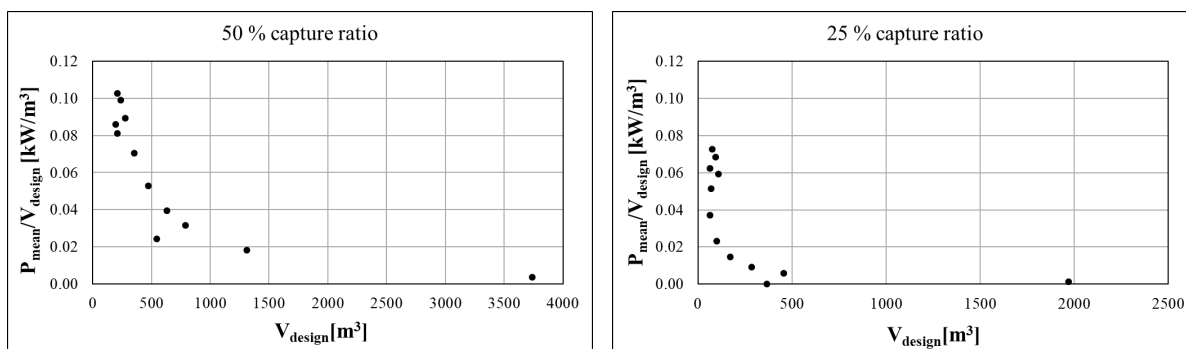
Figure 7. Decreasing the P_{mean}/V_{sub} ratio with increasing the size. Left: 50% capture ratio. Right: 25% capture ratio.

The results are compared with a similar WEC concept in the same site and sea states from Babarit et al. [16] and presented in Table 3. Comparison of the results of the present study with Babarit et al. [4]..It can be seen that the P_{mean} in the present study is considerably higher than that of Babarit et al [4]. This is because the ideal PTO system is considered in the present study while a linear damping passive PTO is used in [4]. However, in [4] the *CWR* and P_{mean}/V_{sub} are much higher compared to the present study. It appears that Babarit et al. [4] aimed to capture the power from all possible sea states which is equivalent to 100% capture ratio. Achieving such capture ratio is not realistic due to the structural limitations of the WEC and PTO system. A more reasonable approach is to design the WEC such that it captures a portion of sea states as defined in this paper by 50% or 25% capture ratio.

Table 3. Comparison of the results of the present study with Babarit et al. [4].

Study	Capture ratio (%)	C_W (m)	CWR (%)	P_{mean} (kW)	P_{mean}/V_{sub} (kW/m³)
Present	50	8.19	1.1	21.5	0.103
Present	25	8.52	1.6	5.5	0.073
Babarit et al. [4]	100	12.6	4.2	2.8	0.9894

4.2. Size paradox

One may have the misunderstanding that larger point absorbers have higher power outputs. The paradox is that the power from point absorbers is not a function of their size. It was mentioned before by Falnes [17] that "small is beautiful" and smaller efficient point absorbers were proposed later by Sjökvist et al. [18]. To illustrate this, three having point absorbers with cylindrical floaters of considerably different sizes are modelled in ANSYS AQWA. As seen from the simulations results in Figure 8, the time-averaged power of the reactive PTO is the same for these three cases.
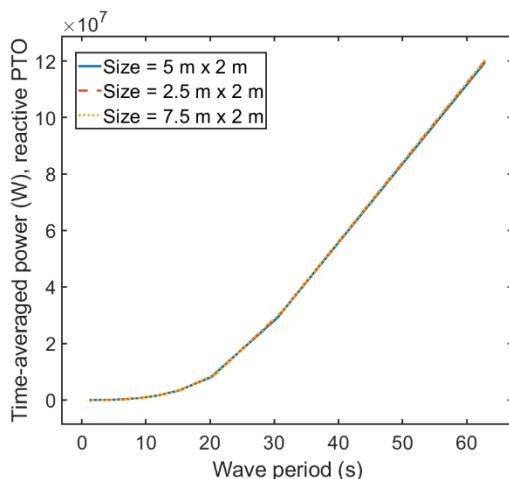

Figure 8. Changes of time-averaged power with wave period.

This phenomenon can be explained by the optimal time-averaged power equation which is a function of excitation force and intrinsic damping (equation (13)).

$$\bar{P}_{PTO,max} = \frac{\left|\hat{F}_e\right|^2}{8\,R_{ins}} \tag{13}$$

As shown in Figure 9, as the size increases, both force amplitude and damping increase. The ratio of the squared force amplitude to the damping coefficient remains nearly the same as shown in Table 4.
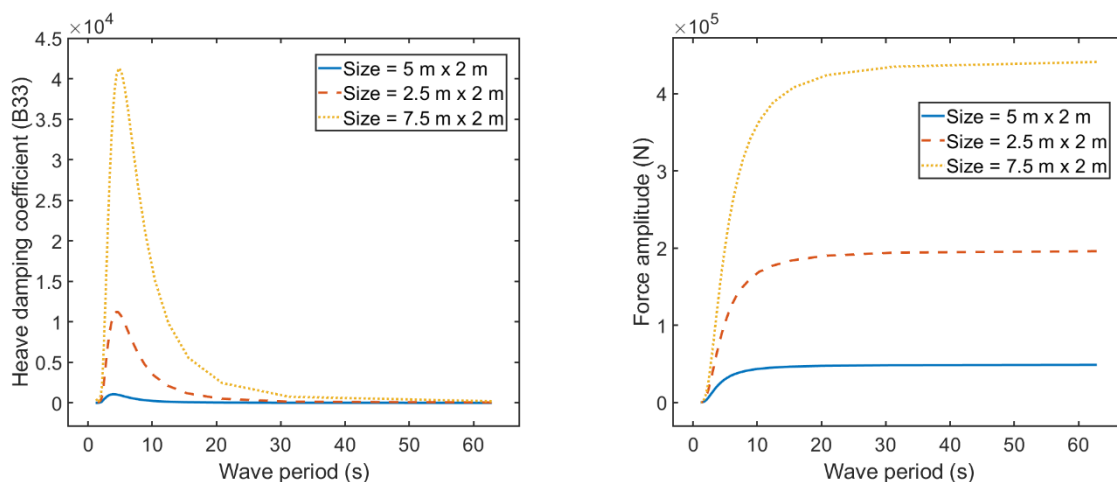

Figure 9. Left: heave damping coefficient vs. wave period. Right: force amplitude vs. wave period.

Table 4. Changes of the force, damping coefficient, and the power with size and wave period.

Wave period (s)	Diameter (m)	Force Amplitude (N)	Damping coefficient (Ns/m)	$\frac{|\hat{f}_e|^2}{8\,R_{ins}}$ (W)
6.0	2.5	34900	738	206302
6.1	5	128000	9030	226800
6.3	7.5	263000	36100	239504

These results confirm the left side Budal upper bound (P_A) in which the power is independent of the volume and is only a function of H and T and therefore the size paradox.

5. Conclusion

In this paper a practical design procedure for initial sizing of heaving point absorbers is proposed. The design procedure starts with determining the the power capture ratio. Next the most optimal set of design wave height (H_{design}) and design wave period (T_{design}) which results in the maximum ratio of mean power to submerged volume (P_{mean}/V_{sub}) is selected. The P_{mean} is calculated by only considering the left-hand Budal curve (P_A). Moreover, the right-hand Budal curve (P_B) and its intersection with the P_A curve is used to find the submerged volume. If the submerged volume corresponding to the highest P_{mean}/V_{sub} ratio is practical, it defines the initial size of the point absorber. The procedure is employed to size a small bottom-referenced heaving point absorber with the sea state data from European Marine Energy Centre by considering two different capture ratios. Then the results are compared with an existing similar point absorber in the same site and show that even with a lower capture ratio, the design procedure leads to a high P_{mean} while keeping a reasonable capture width ratio (CWR). Furthermore, it is shown in that larger point absorbers do not yield higher power and the power is in fact governed by the sea conditions. This is confirmed by modelling point absorbers with considerably different sizes in ANSYS AQWA and plotting their time-averaged power.

References

[1]   Kan M 1979, Wave-power absorption by asymmetric bodies, *Pap. Ship Res. Inst.* **54**, 1-18.
[2]   Haren P and Mei C C 1979, Wave power extraction by a train of rafts: Hydrodynamic theory and optimum design, *Appl. Ocean Res.* **1**(3), 147-157.
[3]   Thomas G P and Gallagher B P 1993, An assessment of design parameters for the Bristol cylinder *Proc. Eur. Wave Energy Symp*. (Edinburgh: Jul 21-24, 1993). p 139.
[4]   Babarit A, Clément A H and Gilloteaux J 2005, Optimization and timedomain simulation of the SEAREV wave energy converter *Proc. 24th Int. Conf. Offshore Mech. Arct. Eng.* (Halkidiki: Jun 12-17, 2005).
[5]   McCabe A P, Aggidis G A and Widden M B 2010, Optimizing the shape of a surge-and-pitch wave energy collector using a genetic algorithm, *Renewable Energy*. **35**(12), 2767-75.
[6]   Bachynski E E, Young Y L and Yeung R W 2012, Analysis and optimization of a tethered wave energy converter in irregular waves, *Renewable Energy*. **48**, 133-45.
[7]   Khojasteh D and Kamali R 2016, Evaluation of wave energy absorption by heaving point absorbers at various hot spots in Iran seas, *Energy*. **109**, 629-40.
[8]   Shadman M, Estefen S F, Rodriguez C A, Nogueira I C M 2018, A geometrical optimization method applied to a heaving point absorber wave energy converter, *Renewable Energy*. **115**, 533-46.
[9]   Erselcana İ Ö and Kükner A 2020, A parametric optimization study towards the preliminary design of point absorber type wave energy converters suitable for the Turkish coasts of the Black Sea, *Ocean Eng*. **218**(108275).
[10]   Falnes J and Hals J 2012, Heaving buoys, point absorbers and arrays, *Philos. Trans. R. Soc. Ser. A.,* **370**, 246-277.

[11]   Budal K and Falnes J 1980, Interacting point absorbers with controlled motion, *Power from Sea Waves*. (London: Academic Press). p 381.

[12]   Murai M, Li Q and Funada J 2021, Study on power generation of single Point Absorber Wave Energy Converters (PA-WECs) and arrays of PA-WECs, *Renewable Energy*. **164**, 1121-32.

[13]   Falnes J 2007, A review of wave-energy extraction, *Mar. struct.* **20**(4), 185-201.

[14]   Falnes J and Kurniawan A 2020, *Ocean Waves and Oscillating Systems: Linear Interactions Including Wave-Energy Extraction* 2nd Ed. (London: Cambridge University Press).

[15]   Nielsen K and Pontes T 2010, *Report T02-1.1 OES IA Annex II Task 1.2 Generic and Site Related Wave Energy Data*. (OES IA: Technical report).

[16]   Babarit A, Hals J, Muliawan M J, Kurniawan A, Moan T and Krokstad J 2012, Numerical benchmarking study of a selection of wave energy converters, *Renewable Energy*. **41**, 44-63.

[17]   Falnes J 1993, Small is beautiful: How to make wave energy economic, *Proc. 1st Int. Symp. Eur. Wave Energy* (Edinburgh: Jul 21-24, 1993) p 367.

[18]   Sjökvist L, Krishna R, Rahm M, Castellucci V, Hagnestål A and Leijon M 2014, On the Optimization of Point Absorber Buoys, *J. Mar. Sci. Eng.* **2**(2), 477-92.